

Spatiotemporal Variation in Tropospheric Column Ozone over East Asia Observed by GOME and Ozonesondes

S. Hayashida¹, N. Urita^{1*}, K. Noguchi¹, X. Liu^{2,3}, and K. Chance²

¹*Faculty of Science, Nara Women's University, Nara, Japan*

²*Atomic and Molecular Physics Division, Harvard-Smithsonian Center for Astrophysics, Cambridge, Massachusetts, USA*

³*Goddard Earth Sciences and Technology Center, University of Maryland, Baltimore, Maryland, USA*

Abstract

We analyzed tropospheric column ozone (TCO) observed by the GOME-1 (Global Ozone Monitoring Experiment; European Space Agency, 1995) and ozonesondes to determine the spatiotemporal variation in TCO over East Asia from 1996 to 2003. An enhanced TCO belt (E-TCO belt) was observed at approximately 35°N throughout the year. The E-TCO belt moved northward from winter to summer and southward from summer to winter, strongly suggesting connection with the seasonal variation of meteorological conditions. The large enhancement of TCO found over central China in summer suggests that there is significant outflow of ozone from that region. This study presents the first satellite-derived comprehensive picture of the TCO spatiotemporal variation over East Asia, which has not been obtained from limited ground-based measurements.

1. Introduction

Tropospheric ozone plays important roles in controlling the chemical composition of the troposphere and influencing the energy budget of the Earth's atmosphere. According to a recent IPCC report (2007), radiative forcing of tropospheric ozone is estimated to be the third most important component among the greenhouse gases. In Asia, recent increases in energy consumption have led to a significant amount of emissions of ozone precursors (Ohara et al. 2007). Therefore, monitoring of spatiotemporal variation of tropospheric ozone over Asia is now of a great concern.

Satellite measurements have the advantage of providing continuous monitoring of ozone over a wide spatial range, thereby allowing the analysis of spatial and temporal variations in ozone over large areas. However, the separation of the relatively small tropospheric component (~10%) from the total column ozone has been difficult. Liu et al. (2005, 2006) derived TCO directly from Global Ozone Monitoring Experiment (GOME) ultraviolet measurements, adapting the spectroscopic technique proposed for GOME and SCIAMACHY measurements (Chance et al. 1997). Noguchi et al. (2007) validated the GOME-O₃ data set by comparing it with ozonesonde data in Japan. In this study, we apply the GOME-O₃ with ozonesonde data from four stations in Japan to determine the spatial distribution and temporal variation in TCO over East Asia.

2. Data analysis

We use version 2 of the GOME-derived TCO data set, retrieved by Liu et al. (2005). The GOME-O₃ version 2 data set is similar to the version 1 data set validated by Noguchi et al. (2007), but has been extended from 2000 to June 2003 after degradation correction of the GOME reflectance spectra, which results from filling voids of the coating of the scan mirror with contaminants (Liu et al. 2007). The spatial resolution of GOME-O₃ is normally 960 × 80 km². We archived the swath data for every orbit onto a 1° × 1° grid and averaged the data by months. Although GOME retrievals derive ozone profiles with 4–7 layers in the troposphere, the retrieved vertical profiles are less reliable in the troposphere (Liu et al. 2005) relative to the integrated TCO. We use only TCO in this study. Tropopause heights from the National Centers for Environmental Prediction (NCEP) reanalysis data were used to determine TCO. We use GOME-O₃ for the period from April 1996 to June 2003, but excluded the period from July 1995 to March 1996.

The ozonesonde data are provided by the Japan Meteorological Agency (JMA) for the four stations of Sapporo (43.1°N, 141.3°E), Tsukuba (36.1°N, 140.1°E), Kagoshima (31.6°N, 130.6°E), and Naha (26.2°N, 127.7°E). For consistency with the GOME data set, we also apply the NCEP-based tropopause heights to the ozonesonde data when deriving TCO.

3. Enhanced TCO belt observed with GOME

The global maps of GOME monthly mean TCO in Fig. 4 of Liu et al. (2006) depict an enhanced TCO belt (hereafter, E-TCO belt) in the mid-latitude Northern Hemisphere (NH), which is particularly evident in summer. Figure 1 shows the GOME TCO maps over East Asia in June and December 1997. Over the area along the Pacific Rim, the E-TCO belt moves northward from winter to summer and southward from summer to winter.

We define the latitude of the belt (L_b) as the latitude where the TCO obtains its maximum value along a longitude. The L_b values between longitudes 125–140°E do not depend significantly on longitude within the area analyzed here. Thus, we consider the L_b value at 130°E to be the representative value for the analyzed area. Figure 2a presents the time-latitude cross-section of TCO along 130°E, with L_b values indicated by dots. Clear seasonal variation in the TCO can be seen in the belt, with a summer maximum and winter minimum. The latitude of the E-TCO belt (L_b) is low (~27°N) in winter and shifts higher (~45°N) in summer.

Figure 2b illustrates the time series of the maximum TCO along 130°E (red), as well as L_b values (blue). The time series of L_b clearly shows that the E-TCO belt reaches its northernmost latitude (L_b at ~40°N) in

Corresponding author: Sachiko Hayashida, Department of Information and Computer Sciences, Faculty of Science, Nara Women's University, Kitauoyanishi-machi, Nara-city 630-8263, Japan. E-mail: sachiko@ics.nara-wu.ac.jp.
*Present affiliation: Mitsubishi Electric Limited, Itami, Japan.
©2008, the Meteorological Society of Japan.

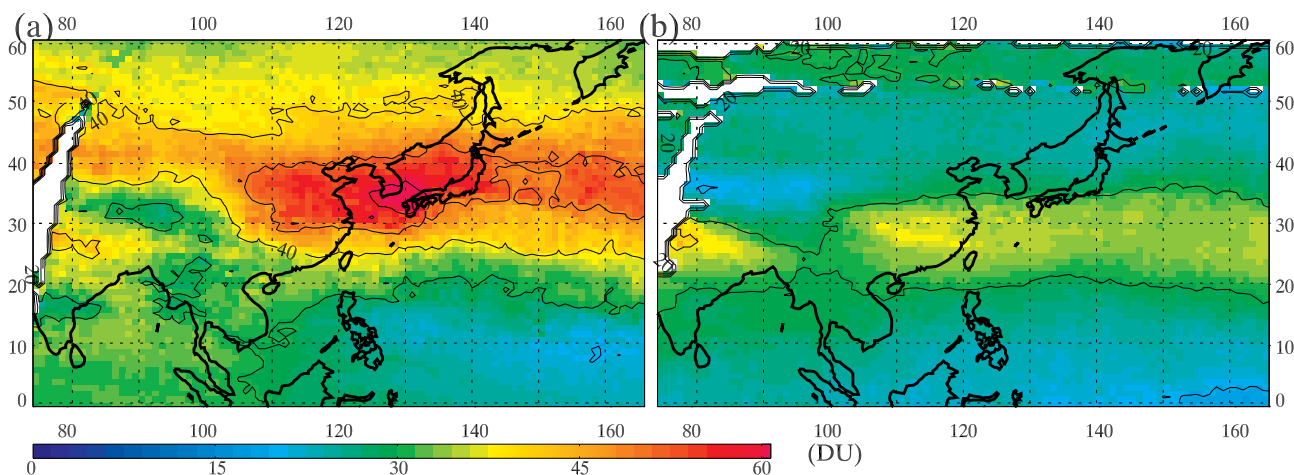


Fig. 1. Maps of GOME monthly mean tropospheric column ozone (TCO) over East Asia in (a) June and (b) December 1997.

August, whereas the maximum TCO is greatest in June. Year-to-year variability can also be seen in the amplitude of the seasonal variation in L_b and maximum TCO.

4. Comparison of seasonal variation in GOME- and ozonesonde-observed TCO

The lower panels of Fig. 2 show time series of ozonesonde-observed TCO at the four stations in Japan (black lines), which are located between 26.2° and 43.1°N (their latitudes are indicated by dotted lines in Fig. 2a). For comparison, GOME-derived TCO values at the same grid with the ozonesonde station are plotted (blue lines). As already reported by Noguchi et al. (2007), the ozonesonde-observed TCO values indicate good correlation with GOME-derived TCO values. The time series of GOME-derived TCO at 130°E and at the latitude of each ozonesonde station are also shown by red lines. Good consistency of red and black lines suggest that ozonesonde-observed TCO values can be interpreted as cross sections of the spatiotemporal picture of the GOME-derived TCO along the dotted lines indicated in Fig. 2a.

Sapporo is located north of the peak latitude of the E-TCO belt throughout the year. Thus, the TCO peak of the belt is not detected at Sapporo. The seasonal variation at Sapporo shows a broad peak in June/July, with the maximum value less than the E-TCO maximum. Tsukuba is located approximately in the middle of the enhanced TCO belt in June; thus, the phase of the seasonal variation at Tsukuba is almost consistent with that of TCO-maximum, but with larger amplitude. Although pollution from nearby Tokyo may occasionally perturb the tropospheric ozone at Tsukuba (Logan 1999), the seasonal variation shown in Fig. 2d is generally as expected at the latitude of Tsukuba. Kagoshima is located at approximately the southern edge of the major part of the E-TCO belt, and the peak season is earlier than in Tsukuba and Sapporo. The southernmost station of Naha shows a pattern well known for the lower latitudes of East Asia, namely a spring maximum and summer minimum (e.g., Liu et al. 2002). The E-TCO belt is situated far north of Naha throughout the year, and the maximum value of the E-TCO belt is not observed there (Figs. 2a,f).

5. Discussion

The retrieval algorithm for TCO uses climatological ozone profiles to initialize and regularize the retrievals (Liu et al. 2006). The retrieved data are similar to a priori data, meaning that the a priori data intrinsically include the seasonal variation in the tropospheric ozone. However, the a priori data are not dependent on longitude and are set to be constant for the years analyzed; therefore, we can consider the spatiotemporal pattern of TCO (Fig. 1) to be its real variation. We have also analyzed the seasonal variation in TCO derived from a combination of Ozone Monitoring Instrument (OMI) and Microwave Limb Sounder (MLS) data (Ziemke et al. 2006). The technique for deriving tropospheric ozone was based on the tropospheric ozone residual (TOR) method. This analysis confirmed that the features of TCO seasonal variation in 2004 and 2005 are similar to those shown in Fig. 2a (figure not shown). The consistency of the two satellite-based data sets and the similarity of the TCO seasonal variation in GOME-O₃ and ozonesonde data (Fig. 2) demonstrate the reliability of the pattern of TCO seasonal variation shown in Fig. 2a.

Previous studies have investigated the seasonal variation in TCO at the four stations in Japan as a combination of transport effects and chemical production/loss processes. Our analysis presented the first satellite-derived comprehensive picture of the TCO spatiotemporal variation over East Asia as indicated in Fig. 2a that has never been obtained before. The time series of the ozonesonde-TCO at each station can be interpreted as a cross section of the spatiotemporal picture of the GOME-derived TCO (Fig. 2a). In other words, the features of seasonal variation in TCO differ at each station based on a combination of the temporal evolution of ozone concentration and the latitudinal shift of the E-TCO belt.

The enhancement of TCO could be attributed to the following three effects: ozone intrusion from the stratosphere; outflow from polluted regions, especially China; and the effect of biomass burning in Southeast Asia (e.g., Liu et al. 2002, Sudo and Akimoto 2007). We have carefully examined TCO values in the lee of central China where the NO₂ concentration is very high (Richter et al. 2005), and found strong enhancement of TCO near the coastline of and over the Yellow Sea, and around Tsushima Island in particular. The ozone enhancement is very likely connected to ozone production in the

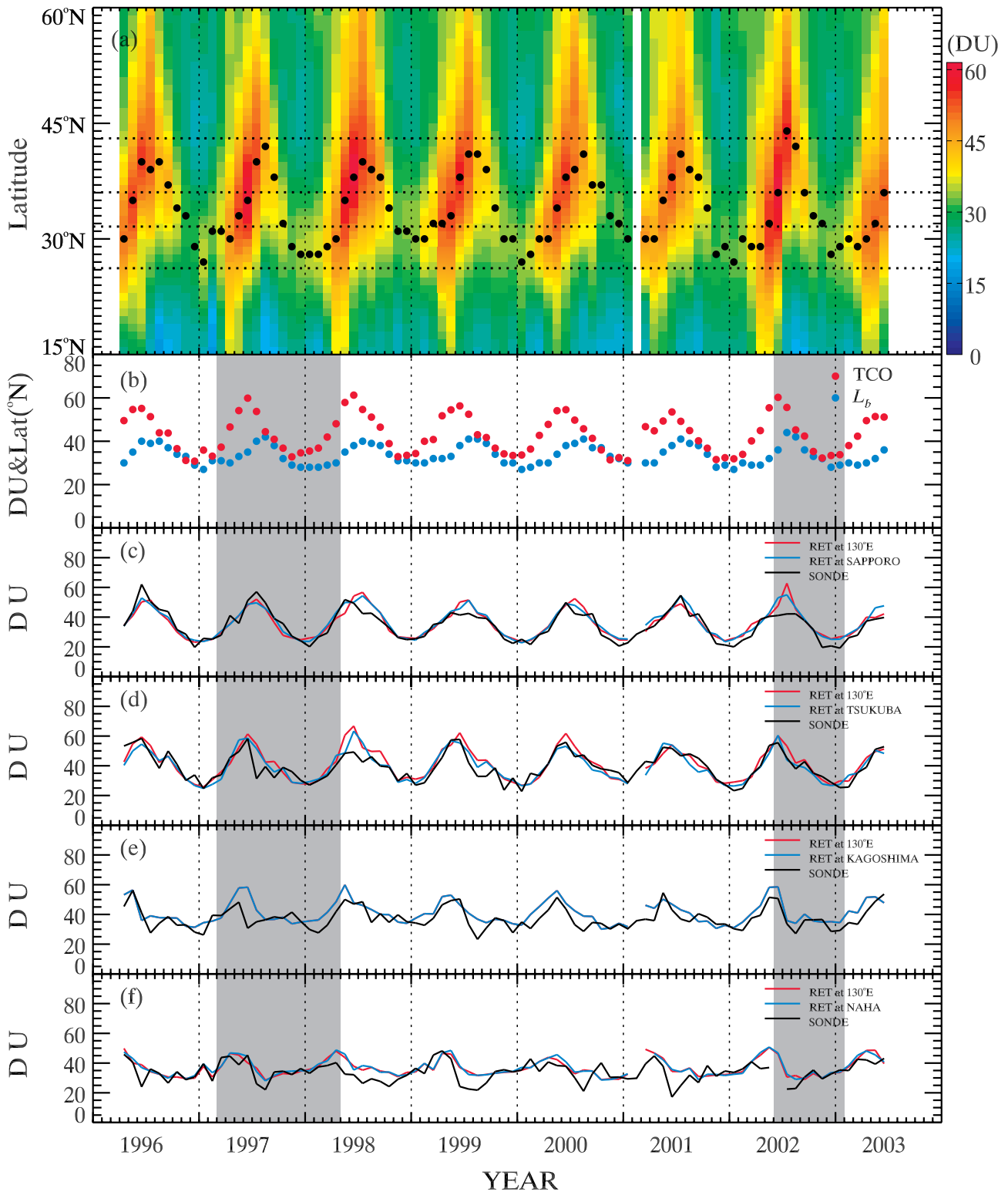


Fig. 2. (a) Time-latitude cross-section of tropospheric column ozone (TCO) along 130°E. Black dots indicate the latitude of the maximum TCO (L_b). Dotted lines correspond to the latitudes of the four ozonesonde stations. (b) Time series of maximum TCO (red), and the latitude of the E-TCO belt (L_b ; blue). (c)–(f): (black) Time series of TCO based on ozonesonde observations at four stations in Japan: (c) Sapporo (43.1°N, 141.3°E), (d) Tsukuba (36.1°N, 140.1°E), (e) Kagoshima (31.6°N, 130.6°E), and (f) Naha (26.2°N, 127.7°E). (red) Time series of GOME- O_3 at 130°E and at the latitude of an ozonesonde station. (blue) Time series of GOME- O_3 at the same grid with the ozonesonde station. For Kagoshima the two time series of GOME- O_3 are identical. Shaded periods refer to El Niño episodes.

polluted air from China or the Korean Peninsula. Some model studies utilized tagged ozone experiments and determined that the monsoonal flow transports Asian ozone towards the northeast in summer in the lower and middle troposphere (e.g., Liu et al. 2002). Zhu et al. (2004) also reported connection of surface ozone over Waliguan station (on the northeastern edge of the Tibetan Plateau) with the monsoon wind system. On the other hand, interannual variability in TCO at low latitude ($\sim 20^\circ\text{N}$) is correlated with the phase of El Niño year (shaded period in Fig. 2), suggesting the effect of biomass burning (Fishman et al. 2005).

Naja and Akimoto (2004) investigated the long-term trends in tropospheric ozone using ozonesonde data collected from four stations in Japan (Naha and Kagoshima, in particular), but they did not find any specific trend in TCO after the 1990s. We confirmed their results by applying a similar approach. However, this study suggests that Naha is not a suitable station to detect the effect of air pollution from China because Naha is located far south of the E-TCO belt. Data from Kagoshima are much more appropriate for such research purposes. However, the approach based on backward trajectory calculations would be insufficient to reveal the ozone trend over East Asia, because the TCO data at the Japanese stations are not always representative over the region through the year. As shown in Fig. 1, the enhancement of TCO depends on latitude, so that some stations may fail to detect the air mass with high ozone in some period in a year. Besides, the most enhanced TCO near Oki and Tsushima Islands (Fig. 1a) is not detected by any ozonesonde measurement. This study suggests that additional ozonesonde measurements at or around Oki Island or Tsushima Island, where the maximum TCO was detected, are desirable to monitor tropospheric ozone over East Asia. It is also suggested that we need a comprehensive data set that includes ground-based and satellite-based measurements to determine the long-term trend of TCO.

6. Summary

We compared GOME- and ozonesonde-TCO at Naha, Kagoshima, Tsukuba, and Sapporo stations in Japan to determine the spatial distribution of and temporal variation in TCO over East Asia. We focused on data from 1996 to 2003 and investigated the seasonal variation in TCO.

Our analysis shows an enhanced TCO belt at approximately 30°N that moves northward from winter to summer and southward from summer to winter, corresponding to the seasonal variation of meteorological condition. The E-TCO belt reaches its northernmost latitude ($\sim 40^\circ\text{N}$) in August, whereas the TCO reaches a maximum in June, when photochemical production is most vigorous. The seasonal variation in TCO derived from ozonesonde measurements is consistent with the behavior of the GOME TCO at the same latitude. Our examination of the outflow of ozone from central China confirms the significant enhancement of TCO over that region. Additional ozonesonde measurements at or around Oki Island or Tsushima Island, where the maximum TCO is found, are desirable to monitor tropospheric ozone, especially as related to air pollution from China and the Korean Peninsula.

References

- Chance, K. V., J. P. Burrows, D. Prener, and W. Schneider, 1997: Satellite measurements of atmospheric ozone profiles, including tropospheric ozone, from UV/visible measurements in the nadir geometry: A potential method to retrieve tropospheric ozone. *JQSRT*, **57**, 467–476.
- European Space Agency, The GOME Users Manual, F. Bednarz, ed., 1995: European Space Agency Publication SP-1182, ESA Publications Division, ESTEC, Noordwijk, The Netherlands.
- Fishman, J., J. K. Creilson, and A. E. Wozniak, 2005: Interannual variability of stratospheric and tropospheric ozone determined from satellite measurements. *J. Geophys. Res.*, **110**, D20306, doi:10.1029/2005JD005868.
- IPCC, 2007: *Climate Change 2007: The Physical Science Basis. Contribution of Working Group I to the Fourth Assessment Report of the Intergovernmental Panel on Climate Change*. Cambridge University Press, UK, 996 pp.
- Liu, H., D. J. Jacob, L. Y. Chan, S. J. Oltmans, I. Bey, R. M. Yantosca, J. M. Harris, B. N. Duncan, and R. V. Martin, 2002: Sources of tropospheric ozone along the Asian Pacific Rim: An analysis of ozonesonde observations. *J. Geophys. Res.*, **107**(D21), 4573, doi:10.1029/2001JD002005.
- Liu, X., K. Chance, C. E. Sioris, R. J. D. Spurr, T. P. Kurosu, R. V. Martin, and M. J. Newchurch, 2005: Ozone profile and tropospheric ozone retrievals from the Global Ozone Monitoring Experiment: Algorithm description and validation. *J. Geophys. Res.*, **110**, D20307, doi:10.1029/2005JD006240.
- Liu, X., K. Chance, C. E. Sioris, T. P. Kurosu, R. J. D. Spurr, R. V. Martin, T.-M. Fu, J. A. Logan, D. J. Jacob, P. I. Palmer, M. J. Newchurch, I. A. Megretskaja, and R. B. Chatfield, 2006: First directly retrieved global distribution of tropospheric column ozone from GOME: Comparison with GEOS-CHEM model. *J. Geophys. Res.*, **111**, D02301, doi:10.1029/2005JD006564.
- Liu, X., K. Chance, and T. P. Kurosu, 2007: Improved ozone profile retrievals from GOME data with degradation correction in reflectance. *Atmos. Chem. Phys.*, **7**, 1575–1583.
- Logan, J. A., 1999: An analysis of ozonesonde data for the troposphere: Recommendations for testing 3-D models and development of a gridded climatology for tropospheric ozone. *J. Geophys. Res.*, **104**(D13), 16115–16149.
- Naja, M., and H. Akimoto, 2004: Contribution of regional pollution and long-range transport to the Asia-Pacific region: Analysis of long-term ozonesonde data over Japan. *J. Geophys. Res.*, **109**, D21306, doi:10.1029/2004JD004687.
- Noguchi, K., N. Urita, S. Hayashida, X. Liu, and K. Chance, 2007: Validation and comparison of tropospheric column ozone derived from GOME measurements with ozonesondes over Japan. *SOLA*, **3**, 41–44.
- Ohara, T., H. Akimoto, J. Kurokawa, N. Horii, K. Yamaji, X. Yan, and T. Hayasaka, 2007: An Asian emission inventory of anthropogenic emission sources for the period 1980–2020. *Atmos. Chem. Phys.*, **7**, 4419–4444.
- Richter, A., J. P. Burrows, H. Nüß, C. Granier, and U. Niemeier, 2005: Increase in tropospheric nitrogen dioxide over China observed from space. *Nature*, **437**, doi:10.1038/nature04092.
- Sudo, K., and H. Akimoto, 2007: Global source attribution of tropospheric ozone: Long-range transport from various source regions. *J. Geophys. Res.*, **112**, D12302, doi:10.1029/2006JD007992.
- Zhu, B., H. Akimoto, Z. Wang, K. Sudo, J. Tang, and I. Uno, 2004: Why does surface ozone peak in summertime at Waliguan? *Geophys. Res. Lett.*, **31**, L17104, doi:10.1029/2004GL020609.
- Ziemke, J. R., S. Chandra, B. N. Duncan, L. Froidevaux, P. K. Bhartia, P. F. Levelt, and J. W. Waters, 2006: Tropospheric ozone determined from Aura OMI and MLS: Evaluation of measurements and comparison with the Global Modeling Initiative's Chemical Transport Model. *J. Geophys. Res.*, **111**, D19303, doi:10.1029/2006JD007089.